ON THE PREDICTION OF THE STRUCTURE
OF INGOTS SOLIDIFYING IN RMF

A. Kapusta[1]*, B. Mikhailovich*[1]*, S. Khripchenko*[2,3]*, I. Kolesnichenko*[2,3]

[1] *Department of Mechanical Engineering, Ben-Gurion University of the Negev,*
P.O.B. 653, Beer-Sheva 8410501, Israel
e-Mail: borismic@bgu.ac.il
[2] *Laboratory of Hydrodynamics, Institute of Continuous Media Mechanics,*
1 Korolev str., Perm 614013, Russia
[3] *Perm National Research Polytechnic University, Russia*

The structure formation of ingots crystallizing from the melt takes place near the crystallization front in boundary layers (namely, in the hydrodynamic boundary layer whose thickness is determined by the melt stirring intensity and temperature and by concentration layers in the case of alloy crystallization), and depends on heat and diffusion fluxes that specify the melt solidification rate. Therefore, we focus here on studying the influence of electromagnetic stirring on heat and momentum transfer near the crystallization front.

Introduction. Magnetohydrodynamic (MHD) stirring has been successfully used to produce ingots with improved mechanical properties. However, the problem of selecting optimal MHD action parameters remains yet unsolved due to the lack of reliable mathematical models that relate the structure of the cast product with the motion of the melt in the vicinity of the solidification front. The likely reason for this is an immense variety of scales used to describe the crystal formation process and melt motion. That is why, the development of mathematical models able to describe macroscopic processes and explain concurrently the influence of hydrodynamic effects on the structure formation of castings and ingots has become increasingly important.

It is known that semi-quantitative information on the structure of castings in the absence of melt stirring can be obtained by computing thermal processes in ingot-mold systems [1]. The authors of this study derived the relationship between the solid phase thickness and the time. For example, as seen in Fig. 1, the solidification velocity curve $dS/d\tau$ for a steel ingot of $700\,\mathrm{mm}$ diameter has four segments, which can be interpreted, with a certain degree of reliability, as charac-
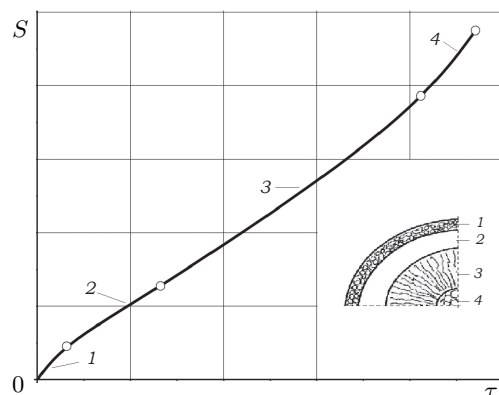
Fig. 1. Diagram of transverse solidification of a cylindrical ingot in the mold and the proper ingot structure (inset). For detailed description see the text.

teristic thicknesses of regions with different macrostructure. Region *1* corresponds to the structure consisting of small close-packed equiaxial crystals (Fig. 1, inset) arising at the initial stage of solidification and is characterized by a maximum heat flux value due to a maximum temperature gradient between the melt and the cold wall of the mold. Region *2* characterizes a transition from a fine-grained structure to a columnar dendritic structure in region *3*. The transition point from region *1* to region *2* can be considered as a point of the critical values of dimensionless thermal parameters characterizing the crystallization front instability at the boundary of region *1*, and region *2* as a transition area from region *1* to region *3*.

Region *3* is characterized by a decrease in heat flux caused by an increase in thermal resistance of the solid phase and a decrease in temperature difference between the crystallization temperature and the growing temperature of the mold. The transition point from region *3* to region *4* indicates the moment when coarse equiaxial crystals begin to grow in the remaining melt volume and the onset of thermal equilibrium between the ingot and the mould, i.e. the moment of transition to the bulk crystallization of the melt.

The electromagnetic impact on the melt during its crystallization gives rise to forced turbulent convection, and this completely changes the fields of temperature and concentration of impurities in the melt and results in the formation of narrow hydrodynamic, temperature and diffusion boundary layers near the interface.

The temperature gradient in the phase transition region thus increases, and the transfer of heat from the melt to the boundary layer becomes more intensive. This assures that the heat flux and, finally, the structure of the crystallized ingot can be controlled by electromagnetic fields.

1. Some general considerations. The ingot structure formation takes place near the crystallization front in the hydrodynamic boundary layer, the thickness of which is determined by the melt stirring intensity, and in the temperature (and concentration, in the case of alloy solidification) boundary layer, whose thickness is related to the intensity of mixing and depends on heat and diffusion fluxes that specify the melt solidification rate. Therefore, our research is concerned the influence of electromagnetic stirring on momentum and heat (and mass, for alloy solidification) transfer processes in the vicinity of the crystallization front. We assume that the absence of the columnar structure of the melt stirred in a rotating magnetic field (RMF) observed in some experiments can be attributed to the occurrence of appropriate conditions that exclude the formation of columnar structure in the temperature boundary layer at some thermal and MHD-parameters, rather than to the mechanical fracture of the structure (as usually explained).

It is unlikely that mathematical models describing the effect of stirring parameters on the generation and development of various structures typical of the crystallization of ingots and castings can be developed in the near future. That is why the emphasis in the present paper is made on theoretical and experimental investigation of critical MHD and thermal conditions generated in the temperature boundary layer under the action of a rotating magnetic field. A detailed analysis of these conditions allows us to produce a reliable estimate of the probability of formation of any (fine-grained equiaxed or columnar) structure.

The foundry technology mainly aims to obtain ingots having a fine equiaxed grain structure without centerline porosity, which provides the improved strength characteristics of cast products. At the same time, castings with a columnar grain structure may be needed in some cases where the anisotropic strength characteristics are important.

474
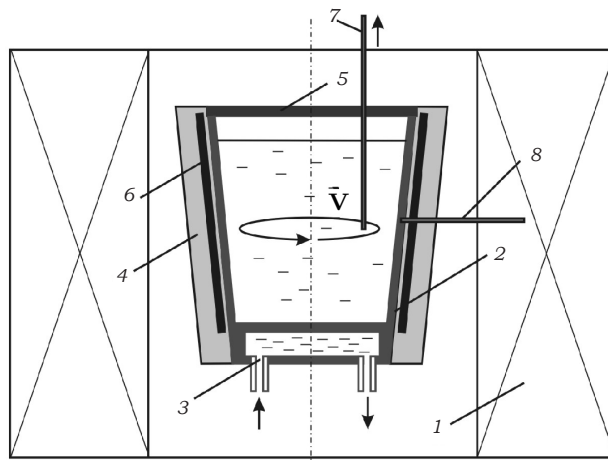
Fig. 2. Scheme of the experimental setup, *1* – MHD stirrer, *2* – mold, *3* – water condenser, *4, 5* – mullite insulation coating and lid, *6* – strip heater, *7* – movable and *8* – fixed thermocouples for melt and wall temperature measuring.

2. Experimental estimates. In order to determine the relationship between the electromagnetic parameters and the heat transfer in the temperature boundary layer, we set up a directional solidification experiment with commercially pure molten tin subjected to MHD stirring in a cylindrical crucible in the presence of a rotating magnetic field.

The experimental setup (Fig. 2) consists of a rotating magnetic field inductor *1* with a bore (diameter 200 mm), where a cylindrical stainless steel mold *2* of a wall thickness of 1 mm (coated from inside with a thin heat-resistant protective layer of special lubricating grease) is placed. The bottom of the crucible is cooled by water condenser *3*. The sidewalls of the mold and its top *5* are thermally insulated with mullite coatings and heated using a 360 W electric heater *6*.

It was assumed that the heater prevented heat from escaping from the sidewalls of the crucible. At a distance of 28 mm from the sidewall of the crucible, we mounted a K-type chromega-alomega sheathed thermocouple *7* (accuracy 0.75%) of 1.6 mm diameter. During the experiment, in which the molten tin was stirred by a rotating magnetic field and crystallized at the bottom of the mold, the thermocouple *7* was automatically raised by a positioning system Isel Automation from the crystallization boundary at a velocity of 1 mm/s. The wall temperature was measured by a fixed thermocouple *8*. Temperature measurements were made with a time interval of 1.3 s. After the thermocouple *7* was raised upwards, it was moved downward again to the solidification front and the process was repeated. This yielded temperature distributions in the liquid phase of the ingot at different moments of time during the directional solidification of the metal subjected to azimuthal MHD stirring. In the course of experiment, we controlled the flow rate of water through the water condenser at the crucible bottom, as well as the temperature of water entering the condenser and leaving it.

3. Problem formulation. Under experimental conditions set up above, the heat flux is calculated as

$$q = -\lambda_{\mathrm{T}} \partial T / \partial z, \tag{1}$$

475

where λ_T is the specific thermal conductivity of the melt. The heat flux in the temperature boundary layer is

$$q_b = -\lambda_T \Delta T/\delta_T, \tag{2}$$

where $\Delta T = T - T_c$, T_c is the crystallization temperature, and δ_T is the thickness of the temperature boundary layer.

In the dimensionless form, the heat flux in the boundary layer can be expressed as

$$\overline{q}_b = -\Delta\theta/\overline{\delta}_T, \tag{3}$$

where $\overline{\delta}_T = \delta_T/R_0$, $\Delta\theta = (T - T_c)/(T_w - T_c)$, T_w is the crucible sidewall temperature, $q_0 = -\lambda_T \Delta T_0/\overline{\delta}_T$, $\Delta T_0 = (T_w - T_c)$.

For melt stirring, the so-called mixed boundary layer thickness $\overline{\delta}_T^*$ [2] can be used instead of $\overline{\delta}_T$:

$$\overline{\delta}_T^* = \int\limits_0^{\overline{\delta}_T} \frac{u(\overline{z})\Delta\theta(\overline{z})}{\langle V_0 \rangle}\, \mathrm{d}\overline{z}, \tag{4}$$

where $u(\overline{z}) = (\mathrm{Ha}/\beta)^2(1 - \mathrm{e}^{-\chi z})$, $\chi = \delta_z\beta$, $\delta_z = Z_0/R_0$, $\beta = \sqrt{\lambda + \mathrm{Ha}^2 K_a}$, $\lambda = C_\varepsilon(\mathrm{Re}_\omega\Omega)^{1-\varepsilon}/\delta_z$ is the "external" friction coefficient [3], Ω_z is the angular velocity of melt rotation in the flow core, Z_0 is the height of the melt column, R_0 is the inner radius of the cylinder (casting mold), $K_a = 1 - \mathrm{th}\delta_z/\delta_z$ is the attenuation coefficient [4]. The Hartmann number $\mathrm{Ha} = B_0 R_0\sqrt{\sigma/\rho\nu}$ is based on the imposed magnetic field and on the melt conductivity, density and viscosity σ, ρ, ν; the Reynolds number $\mathrm{Re}_\omega = \omega R_0^2/\nu$ is built on the angular velocity ω. The experimentally determined parameter $C_\varepsilon = C_0\mathrm{e}^{11.545\varepsilon}$ where $C_0 = 0.0487$.

After integrating Eq. (4), taking into account the smallness $\overline{\delta}_T\mathrm{e}^{-\chi\overline{\delta}_T}/(2\chi)$, we have

$$\overline{\delta}_T^* = \overline{\delta}_T^2 + \overline{\delta}_T/(2\chi), \tag{5}$$

hence, we can find the relation between the characteristic size of the temperature layer and that of the mixed boundary layer

$$\overline{\delta}_T = \frac{\sqrt{1 + 4\chi^2\overline{\delta}_T^*} - 1}{4\chi}. \tag{6}$$

The MHD flow of the melt under the action of RMF is analyzed in terms of the "external" friction model [3], which relates the change in flow regime with various values of the structural parameter ε. The model is based on the analysis of numerous experimental data which indicate that the character of variation of the angular velocity in the melt flow core changes abruptly at certain critical values of the Hartmann and Reynolds numbers. This, in turn, demonstrates an abrupt change in flow structure, to which a specified value of the parameter ε corresponds. In particular, it has been found that the most probable values of the structural parameter ε are concentrated near $+1$, 0 and -1. The "external" friction model has been developed to describe the rotational laminar, transitional and turbulent MHD flows. It stems from the Navier-Stokes equation, where the nonlinear term $(\mathbf{V}\nabla)\mathbf{V}$ is replaced by the quasi-linear term $\lambda\mathbf{V}$.

In the dimensionless form, the equation of motion for the azimuthal component of the flow is written in the form:

$$\mathrm{Re}_\omega\frac{\partial V_\varphi}{\partial\tau} = \hat{L}V_\varphi - \beta^2 V_\varphi + \mathrm{Ha}^2 r K_a, \tag{7}$$

where

$$\hat{L} = \frac{\partial^2}{\partial r} + \frac{1}{r}\frac{\partial}{\partial r} - \frac{1}{r^2} + \frac{1}{\delta_z^2}\frac{\partial^2}{\partial z^2};$$

r, φ, z denote cylindrical coordinates.

Eq. (7) with the boundary conditions of the 1st or 2nd kind is solved. The characteristic values of the quantities are $V_0 = \omega R_0$, $\tau_0 = 2\pi/\omega$, where ω is the angular current velocity in the RMF inductor with one pair of poles ($p = 1$).

For the steady-state flow in the cylinder, when $\partial V_\varphi/\partial \tau = 0$, Eq. (7) with the boundary conditions $V_\varphi|_{r=1} = 0$ and $V_\varphi|_{r=0} < \infty$ has the following solution:

$$V_\varphi = \frac{\mathrm{Ha}^2}{\beta^2}\left[r - \frac{I_1(\beta r)}{I_1(\beta)}\right], \tag{8}$$

where $I_1(\beta r)$, $I_1(\beta)$ are the modified Bessel functions of the first kind.

According to Eq. (8), the profile of the azimuthal velocity component is linear over the entire domain excluding a thin boundary layer on the mold sidewall, whose dimensional thickness is

$$\delta_r \sim: \beta^{-1} \tag{9}$$

Besides, by solving Eq. (8) it follows that the angular velocity of melt rotation in the flow core is independent of the coordinates r and z

$$\Omega_z = \frac{\mathrm{Ha}^2}{\beta^2} = f(\mathrm{Ha}, \mathrm{Re}_\omega, \delta_z, \varepsilon). \tag{10}$$

In virtue of Eq. (10), we can derive the universal formula to relate the angular core rotation velocity and the MHD parameters for any values of the structural parameter ε:

$$\frac{\Omega_z^{2-\varepsilon}}{1 - \Omega_z} = Q_\varepsilon, \tag{11}$$

where

$$\Omega_\varepsilon = \frac{\mathrm{Ha}^2 \delta_z K_\mathrm{a}}{C_\varepsilon \mathrm{Re}_\omega^{1-\varepsilon}}. \tag{12}$$

4. Analysis of calculated and experimental data. According to Eqs. (11) and (12), we can write for $\varepsilon = 1$:

$$Q_1 = \frac{\mathrm{Ha}^2 \delta_z K_\mathrm{a}}{C_1}, \quad C_1 = 0.0487\mathrm{e}^{11.545} = 5028.74, \tag{13}$$

where

$$\Omega_1 = \frac{Q_1}{Q_1 + 1}; \tag{14}$$

for $\varepsilon = 0$:

$$Q_0 = \frac{\mathrm{Ha}^2 \delta_z K_\mathrm{a}}{C_0 \mathrm{Re}_\omega}, \tag{15}$$

where

$$\Omega_0 = 0.5 Q_0 \left(\sqrt{1 + 4/Q_0} - 1\right). \tag{16}$$

Using formulas (13)–(16) and basing on the experimental MHD action parameters, three critical values of the Hartmann number have been found. It is shown that the azimuthal velocity component changes in the transition stirring mode as well as in the turbulent one, which occurs at Hartmann numbers greater than the critical values (Figs. 3–5).
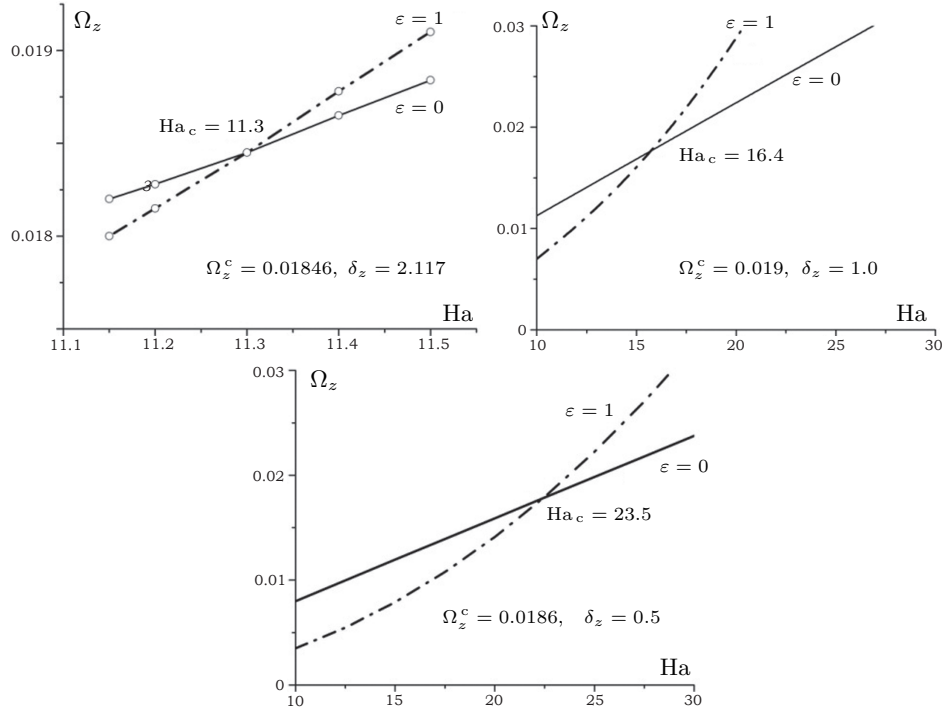
Fig. 3. Dimensionless angular velocity of melt rotation as a function of the Hartmann number at the onset of crystallization (Fo $= 0$).

For better understanding of the process of melt crystallization in the RMF, we have to consider the relationship shown in Fig. 4, which characterizes the change of flow regimes during solidification. Fig. 5 shows the time variation of the melt flow regime at critical values of the MHD parameters.

During melt solidification in a sufficiently strong RMF (Ha ≥ 12), the turbulent flow regime ($\varepsilon = 0$) is initially transformed into the transitional non-laminar regime ($\varepsilon = 1$). In first 280 seconds (Fig. 5), the melt flow regime is turbulent, which provides the intensive heat transfer into the boundary layer at Ha $= 16.92$. Further, the flow regime changes, which leads to a drastic decrease of the heat flow and produces conditions for the growth of columnar crystals. The dependence of the angular rotation velocity of the melt on the Fourier criterion Fo $= at/Z_0^2$ can be calculated using the following formulas:

$$Q_1 = \frac{\mathrm{Ha}^2 \delta_{z0} K_{\mathrm{a}}}{5028.74} \left(1 - \frac{\mathrm{Pr}}{\delta_z}\mathrm{Fo}\right) \quad \text{for} \ \ \varepsilon = 1, \tag{17}$$

$$Q_0 = \frac{\mathrm{Ha}^2 \delta_{z0} K_{\mathrm{a}}}{0.0489 \mathrm{Re}_\omega} \left(1 - \frac{\mathrm{Pr}}{\delta_z}\mathrm{Fo}\right) \quad \text{for} \ \ \varepsilon = 0, \tag{18}$$

where Re $= f(\mathrm{Ha}, \mathrm{Re}_\omega) = \langle u_z \rangle R_0/\nu$, Pr $= \nu/a$, t is the dimensional time, a is the thermal diffusivity.

As the Hartmann number approaches the critical value, the duration of the turbulent flow regime is greatly reduced. To estimate the thickness of the hydrodynamic boundary layer at the bottom of the vessel (near the front of crystallization upon cooling the vessel bottom), we turn to Eq. (7). Since the theory and experiments indicate that the azimuthal melt flow velocity in the core increases linearly
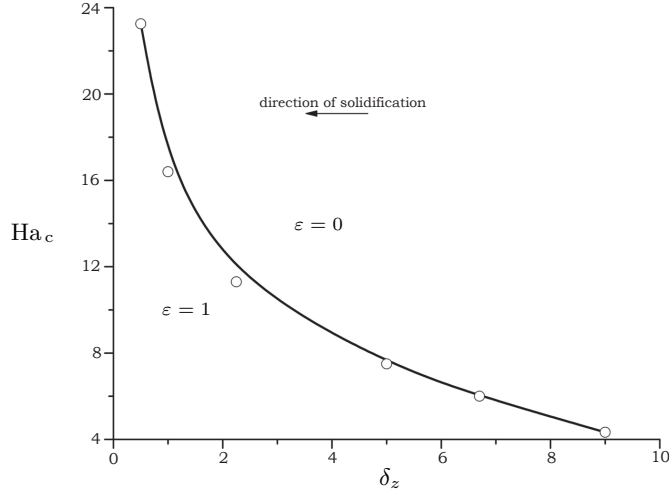
Fig. 4. Critical values of Ha vs. δ_z. The curve divides the region in two domains with different flow regimes: transitional ($\varepsilon = 1$) and turbulent ($\varepsilon = 0$). Three lower points are experimental data obtained from the test with pure tin, and three upper points are calculated data.
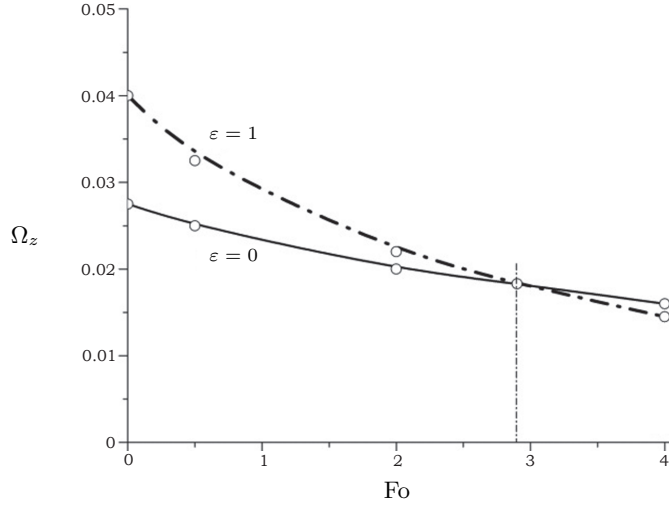
Fig. 5. Dimensionless angular velocity of melt rotation as a function of the Fourier criterion for two different values of ε, and determination of the point of transition from turbulent ($\varepsilon = 0$) to transitional non-laminar ($\varepsilon = 1$) flow regime; Ha = 16.92, Re$_\omega$ = 5596040.

with the radius, the action of the operator $\hat{L}$ nullifies the terms associated with the radius, and Eq. (7) is transformed as

$$\frac{\mathrm{d}^2\Omega_z}{\mathrm{d}z^2} - \chi^2\Omega_z = -\delta_z^2\mathrm{Ha}^2. \tag{19}$$

Boundary conditions of Eq. (19) are as follows:

$$\left.\Omega_z\right|_{z=0(\delta_{zs})} = 0, \quad \left.\Omega_z\right|_{z=\delta_T} = \frac{\mathrm{Ha}^2}{\beta^2}. \tag{20}$$

479
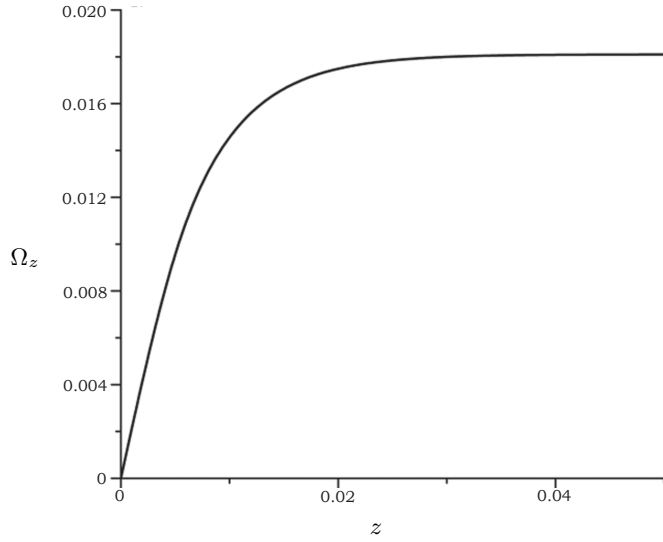
Fig. 6. Thickness estimation of the hydrodynamic boundary layer above the interface. Changes in dimensionless angular velocity of melt rotation along a normal to the crystallization front; Ha = 11.2.
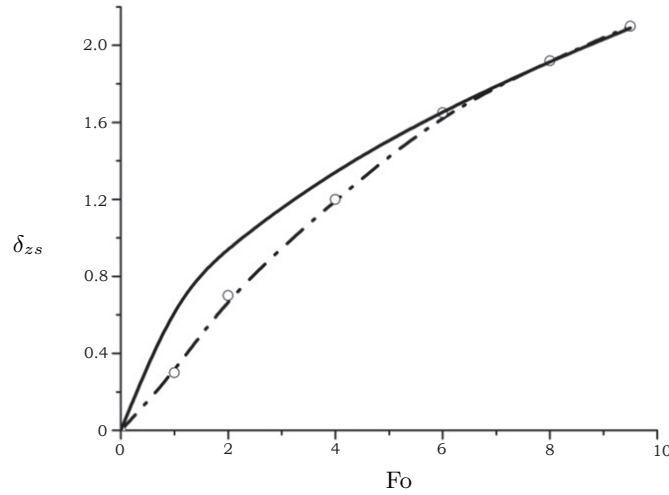
Fig. 7. Dimensionless thickness of the crystallizing ingot as a function of the Fourier criterion: solid curve calculated by formula (23); dashed curve – tin experiment.

A solution to Eqs. (19)–(20) takes the form:

$$\Omega_z = \frac{\text{Ha}^2}{\beta^2} \left\{ \left[\frac{2 - e^{-\chi\delta_T}}{2\text{ch}(\chi\delta_T)} - 1 \right] e^{-\chi z} - \frac{2 - e^{-\chi\delta_T}}{2\text{ch}(\chi\delta_T)} e^{\chi z} + 1 \right\}. \tag{21}$$

Since $1/\text{ch}(\chi\delta_T) \to 0$ solution (21) can be written as (see Fig. 6):

$$\Omega_z = \frac{\text{Ha}^2}{\beta^2} \left(1 - e^{-\chi z} \right). \tag{22}$$

The dynamics of the solid phase growth in the case of directional crystallization of the tin ingot of mean diameter $D = 0.12\,\text{m}$ and length $h = 0.127\,\text{m}$ is

shown in Fig. 7. The upper curve is calculated by the formula

$$\delta_{zs} = 1.832\sqrt{\frac{\text{Fo}}{1 + 3\kappa_{\text{c}}}} \tag{23}$$

and describes the solidification of the ingot in the absence of stirring [1] (here $\kappa_{\text{c}} = q_{\text{c}}/(c\Delta T)$, where q_{c} is the crystallization heat and c is the specific heat).

The experimental curve obtained for the ingot subject to the RMF (MHD stirring of pure molten tin) during ingot solidification is, as expected, shifted relative to the calculated curve.

In our case, the Ficks second equation (thermal diffusion equation) expressed in the dimensionless form has the form is

$$\frac{\partial\theta}{\partial\text{Fo}} - \frac{\text{Pe}}{\delta_{z0}}\frac{\partial\theta}{\partial z} = \frac{1}{\delta_z^2}\frac{\partial^2\theta}{\partial z^2}, \tag{24}$$

where $\text{Pe} = u_z R_0/a$ is the Peclet number; the term

$$\frac{\text{Pe}}{\delta_{z0}}\frac{\partial\theta}{\partial z}$$

in the last equation describes the influence of the convective heat transfer on the process of ingot solidification, and the term

$$\frac{1}{\delta_z^2}\frac{\partial^2\theta}{\partial z^2}$$

is the heat transfer due to thermal conductivity.

The experimental curve in Fig. 7 shows that for the Fourier number $0 < \text{Fo} \leq 3$ the convective heat transfer dominates over the diffusion transfer. In this case, the inequality

$$\frac{\text{Pe}}{\delta_{z0}}\frac{\partial\theta}{\partial z} > \frac{1}{\delta_z^2}\frac{\partial^2\theta}{\partial z^2}$$

should be fulfilled. In the first approximation, by eliminating the diffusion term in Eq. (24), we obtain

$$\frac{\partial\theta}{\partial\text{Fo}} = \frac{\text{Pe}}{\delta_{z0}}\frac{\partial\theta}{\partial z}. \tag{25}$$

Hence, taking into account the linear behavior of the experimental curve at the initial segment and replacing the derivatives by the finite differences yield

$$\Delta z \simeq \frac{\text{Pe}}{\delta_{z0}}\Delta\text{Fo}. \tag{26}$$

The experimental curve (Fig. 7) and relation (26) allow us to evaluate the value of the Peclet number. In this case,

$$\text{Pe} \simeq \frac{\delta_{z0}\Delta z}{\Delta\text{Fo}} = \frac{2.117 \cdot 0.95}{3} = 0.67, \tag{27}$$

and convective term in Eq. (24) with accuracy up to the factor $\Delta\theta$ is

$$\frac{\text{Pe}}{\delta_{z0}\Delta z} = 0.333, \tag{28}$$

and the diffusion term is

$$(\delta_{z0}\Delta z)^{-2} = 0.247. \tag{29}$$
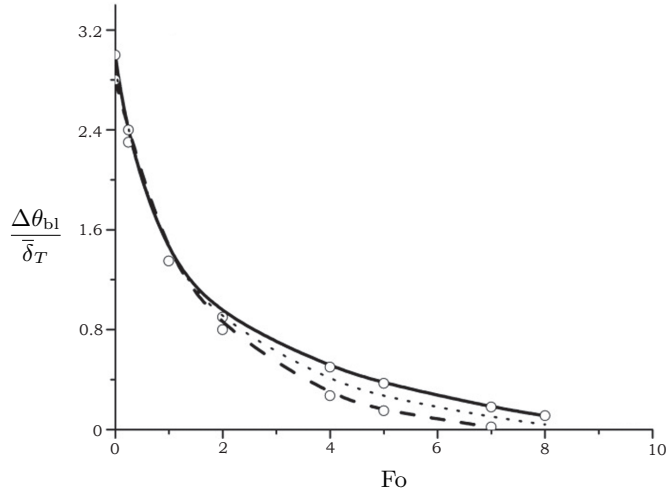
Fig. 8. Dimensionless temperature gradient in the thermal boundary layer as a function of the Fourier criterion, $\mathrm{Ha} = 11.28 < \mathrm{Ha_c}$: dashed curve: along the z-axis of the mold, solid curve: $30\,\mathrm{mm}$ to the axis; dotted curve: average values (see detailed description in the text).
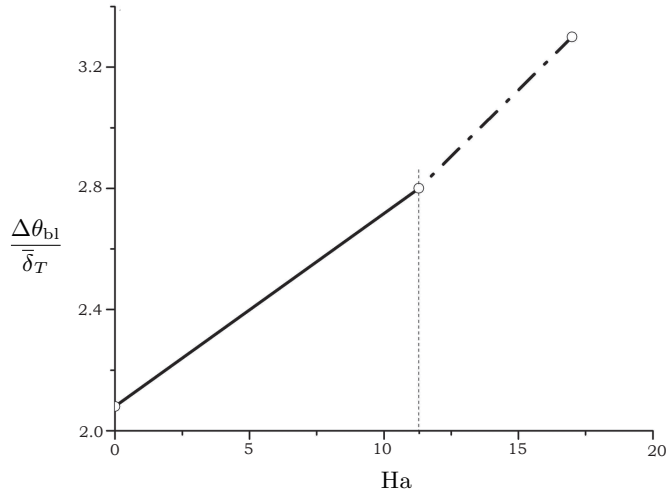
Fig. 9. Dimensionless temperature gradient in the boundary layer as a function of the Hartmann number along the axis of the crucible at the onset of crystallization at $\mathrm{Re}_\omega = 5.596 \cdot 10^6$, $\mathrm{Ha_c} = 11.3$, $\delta_z = 2.117$; dashed line corresponds to expected change in the temperature gradient at $\mathrm{Ha} > \mathrm{Ha_c}$.

According to the determined value of the Peclet number and estimate (27), we can evaluate the z-component of the melt flow velocity in the boundary layer: $\langle u_z \rangle \simeq a\mathrm{Pe}/R_0 = 2.4 \cdot 10^{-4}\,\mathrm{m/s}$ (note that computer simulation yields close values $\langle u_z \rangle = 2.5 \cdot 10^{-4}\,\mathrm{m/s}$).

As the melt solidifies, the curves in Fig. 7 approach each other. The point is that the melt flow velocity decreases, and the intensity of convective transfer is reduced compared to diffusion transfer. Further cooling of an ingot after its full solidification is determined by its thermal conductivity and the rate of heat extraction.

The experimental curves in Fig. 8 are characterized by a decrease in dimensionless heat flow during solidification of the melt stirred in the RMF for the Hartmann number Ha = 11.28, which is typical of the transition regime near the point of transition to the turbulent flow, which is realized at the critical Hartmann number Ha_c. The averaged (dotted) curve is approximated well by the formula $\Delta\theta/\bar\delta_T \approx 2.8\mathrm{e}^{-0.5\text{Fo}}$. Here, $\Delta\theta_{\text{bl}} = (T_{\text{bl}} - T_{\text{c}})/(T_{\text{w}} - T_{\text{c}})$; T_{bl} is the temperature of the external edge of the boundary layer; $T_{\text{w}} = 370°\text{C}$ is the temperature of the crucible wall; $T_c = 232°\text{C}$ is the temperature of tin crystallization; $\theta = (T_{\text{w}} - T)/(T_{\text{w}} - T_{\text{c}})$; $\text{Fo} = 10.3 \cdot 10^{-3}t$ (t in seconds); δ_T is measured from the bottom of the mold.

The character of changes in heat flux within the interval of values $0 < \text{Fo} \le 0.5$ is attributed to the heat extraction; further reduction in heat flux is likely due to the formation of an air gap between the ingot and the bottom of the crucible and to the heating of the sidewall of the crucible.

Fig. 9 illustrates one of the important stages of our investigation – determination of the direct relation between the dimensionless heat flux in the temperature boundary layer and the dimensionless MHD parameters: the numbers Ha and Re_ω which define the intensity of electromagnetic stirring of the melt and its influence on the structure of a crystallizing ingot.

Conclusions. Based on the experiments with liquid metal in a rotating magnetic field, the ability to control the structure of solidifying ingots in relation to the heat flux in the temperature boundary layer was evaluated.

Calculations of critical values of the basic MHD parameters (Ha and Re_ω) determining the structural transition between turbulent and non-turbulent regimes of the melt flow were performed. The character of changes in the thermal processes taking place in the temperature boundary layer during the structural transition was analyzed. The effect of changes in constitutive MHD parameters on the value of heat flux in the temperature boundary layer was evaluated.

The estimates obtained provide a promising tool to establish the relationship between the structure of the ingot solidified in a rotating magnetic field and the constitutive MHD parameters (i.e. the intensity of stirring) and to manipulate the process of crystallization in order to obtain ingots with enhanced structure.

REFERENCES

[1] E.M. GOLDFARB. *Heat Engineering of Metallurgical Processes* (Moscow, Metallurgy 1967). (in Russ.).

[2] L.G. LOITSYANSKY. *Laminar Boundary Layer* (Fizmatgiz, Moscow, 1962), p.309. (in Russ.).

[3] A. KAPUSTA, B. MIKHAILOVICH. On soft stability loss in rotating turbulent MHD flows. *Fluid Dynamics Research*, vol. 46 (2014), p. 041416; doi:10.1088/0169-5983/46/4/041416.

[4] A.I. VOLDEK. *Induction Magnetohydrodynamic Machines with a Liquid Metal Working Body* (Army Foreign Science and Technology Center Charlottesville VA, USA, 1974).